

Journal of Materials Chemistry A

Accepted Manuscript



This is an *Accepted Manuscript*, which has been through the Royal Society of Chemistry peer review process and has been accepted for publication.

Accepted Manuscripts are published online shortly after acceptance, before technical editing, formatting and proof reading. Using this free service, authors can make their results available to the community, in citable form, before we publish the edited article. We will replace this *Accepted Manuscript* with the edited and formatted *Advance Article* as soon as it is available.

You can find more information about *Accepted Manuscripts* in the [Information for Authors](#).

Please note that technical editing may introduce minor changes to the text and/or graphics, which may alter content. The journal's standard [Terms & Conditions](#) and the [Ethical guidelines](#) still apply. In no event shall the Royal Society of Chemistry be held responsible for any errors or omissions in this *Accepted Manuscript* or any consequences arising from the use of any information it contains.

Cite this: DOI: 10.1039/c0xx00000x

ARTICLE TYPE

www.rsc.org/xxxxxx

A novel structured catalyst: gold supported on thin bimetallic (Ni, Co) carbonate hydroxide nanosheet arrays †

Wenxian Liu, Xiwen Weng, Qiu Yang, Tian Li, Junfeng Liu* and Xiaoming Sun

Received (in XXX, XXX) XthXXXXXXXXXX 200X, Accepted Xth XXXXXXXXXXXX 200X

DOI: 10.1039/b000000x

Thin bimetallic (Ni, Co) carbonate hydroxide nanosheet arrays (NiCoCH-NSAs) were successfully synthesized by a two-step hydrothermal method, and used as supports of Au nanoparticles aiming to the application of structured catalysts. The unique architecture of such bimetallic carbonate hydroxide nanosheet with average thickness of about 50 nm and length of 1.5 μm is beneficial to the deposition of small Au nanoparticles without aggregation. HRTEM results clearly showed that the gold nanoparticles with size of about $2.6 \text{ nm} \pm 0.7 \text{ nm}$ were uniformly distributed across the surface of the NiCoCH-NSAs over a large area. As a model reaction, the reduction of p-nitrophenol (4-NP) by sodium borohydride (NaBH_4) was used to evaluate the performance of Au/NiCoCH-NSAs catalysts. The obtained results demonstrated that the as-prepared Au/NiCoCH-NSAs exhibited excellent catalytic activity and stability in the reduction of 4-NP. Notably, the catalytic conversion of 4-nitrophenol in a relatively large scale showed the potential of Au/NiCoCH-NSAs as a practical catalyst for industrial applications. In addition, Au/NiCoCH-NSAs could be easily recycled due to the unique architectures of nanoarrays.

1 Introduction

The gold nanoparticles have attracted extensive attentions due to their optical and electronic properties and potential utility in catalysis.^{1,2} In particular, catalysis by gold has been a hot topic in chemistry since the pioneering demonstrations of supported Au nanoparticles as extraordinarily good catalysts in low-temperature CO oxidation.³⁻⁵ The improvement of the catalytic efficiency and the reduction of the used amounts of gold are the top priorities for practical applications due to its high cost and limited supply.⁶ In order to obtain high catalytic efficiency, Au nanoparticles are generally dispersed on support materials and their catalytic performances are thus highly dependent on the structure and properties of supports, in addition to the inherent properties of gold and its dimension and morphology.^{7,8} Au nanoparticles with small size have highly active surface atoms, however, often tend to aggregate during catalysis and therefore lead to a rapid decay in their catalytic activities. Thus, much attention has been focused on the synthesis of small sized and highly dispersed Au nanoparticles. However, the complicated post-treatment processes make it difficult to obtain small sized and highly dispersed Au nanoparticles.⁹

On the other hand, most of supported gold catalysts are based on particle supports, which could cause flow maldistribution, hot-spots formation and high dispersion in the residence time distribution in traditional industrial reactors.^{10,11} In this regard, the reactor with structured catalyst is considered as a valuable

alternative to solve these problems, which provides small pressure drop, controllable mass transport, good thermal and mechanical properties in the reaction, leading to a higher efficiency and selectivity of the reaction. It is beneficial for the environment and also from the energy economic point of view. In addition, structured catalyst shows the advantages of easy separation and recyclability compared with conventional particle catalysts.^{10,12-14} In recent years, Au nanoparticles have been immobilized onto the various supports such as polymer,¹⁵ graphene hydrogel,¹⁶ carbon nanotube¹⁷ and tin oxide,¹⁸ etc. These well-controlled structured catalysts can stabilize Au nanoparticles against sintering, resulting relatively high catalytic efficiency. However, these structured catalysts sometimes have the drawback of low mechanical stability and low loading surface area. Nanoarrays, which have been demonstrated to be the optimized architecture for electrochemical electrodes,¹⁹⁻²² offer the possibility to fabricate novel structured catalysts with high reactivity and stability.¹² The unique design of nanoarrays, which are commonly constructed by directly growing one-dimensional (1D) or two-dimensional (2D) building blocks upon substrates, has many merits required for high performance structured catalyst, such as large active surface area, high utilization efficiency of active materials, and superior mass transport property.^{23,24} However, little work has been focused on the nanoarrays supported Au structured catalysts.

Herein, we report the successful fabrication of the thin bimetallic (Ni, Co) carbonate hydroxide nanosheet arrays (NiCoCH-NSAs) by a two-step hydrothermal method, and the

use of the NiCoCH-NSAs as supports to deposit and stabilize gold nanoparticles to prepare the Au/NiCoCH-NSAs through deposition reduction method. The content of Au on the nanosheet arrays could be well controlled by changing the amount of the reactants. The catalytic experiments indicated that the as-prepared Au/NiCoCH-NSAs have excellent catalytic activity and stability in the reduction of p-nitrophenol (4-NP) by NaBH₄, even for highly concentrated 4-NP. Moreover, the construction of Au/NiCoCH-NSAs in a structured way allows the catalyst to be easily separated from the reaction mixture and recycled, which makes them potential candidates for industrial applications.

2 Experimental section

2.1 Synthesis of NiCoCH-NSAs

All chemicals were analytical grade, and all solutions were prepared with deionized water. The procedure for the synthesis of NiCoCH-NSAs consists of two hydrothermal reactions. In a typical synthesis, 2 mmol Co(NO₃)₂·6H₂O, 8 mmol NH₄F, and 10 mmol CO(NH₂)₂ were dissolved in 40 mL of deionized water under stirring. The as-prepared homogeneous solution was transferred into a Teflon-lined stainless steel autoclave. Nickel foams (2.0 cm×4.0 cm) were carefully cleaned with HCl (1 M), absolute ethanol, and distilled water. After the cleaned nickel substrate was immersed in the homogeneous solution, the autoclave was sealed and maintained at 120°C for 12 h and then allowed to cool down to room temperature naturally. After being washed with distilled water and dried at 70°C for 2 h, bimetallic (Ni, Co) carbonate hydroxide nanowire arrays (NiCoCH-NWAs) could be obtained.²¹ For preparing NiCoCH-NSAs, 1 mmol Co(NO₃)₂·6H₂O and 10 mmol CO(NH₂)₂ were dissolved in 40 mL of deionized water in a Teflon-lined stainless steel autoclave under stirring. Then, the NiCoCH-NWAs obtained above were immersed in the homogeneous solution, and the autoclave was sealed and maintained at 100°C for 10 h. After the autoclave was cooled to room temperature, the samples were washed with distilled water and dried at 70°C for 2 h to prepare the NiCoCH-NSAs.

2.2 Synthesis of Au/NiCoCH-NSAs

Au/NiCoCH-NSAs were fabricated using NiCoCH-NSAs as supports and HAuCl₄ as the gold source through a deposition reduction method.²⁵ In a typical synthesis, HAuCl₄ solution (0.048 M) and sodium citrate solution (0.01 M) were added into a beaker containing 40 mL of deionized water under stirring. Then the NiCoCH-NSAs (0.065 g) on Ni foam was immersed into the above solution, and then fresh NaBH₄ (0.01 M) was added. After slowly stirring for 1 h, the sample was taken out, washed with deionized water for several times to remove residual ions and molecules, and then dried at 70°C for 2 h. Four samples of Au/NiCoCH-NSAs with different loading amounts of gold (0.1, 0.7, 2.8, 8.1 wt%) were fabricated. For each sample, the adding amount of HAuCl₄ solution was 5 μL, 50 μL, 200 μL, 600 μL, respectively and the amount of sodium citrate solution and sodium borohydride solution to HAuCl₄ solution were kept to 1: 2 by volume.

2.3 Characterization

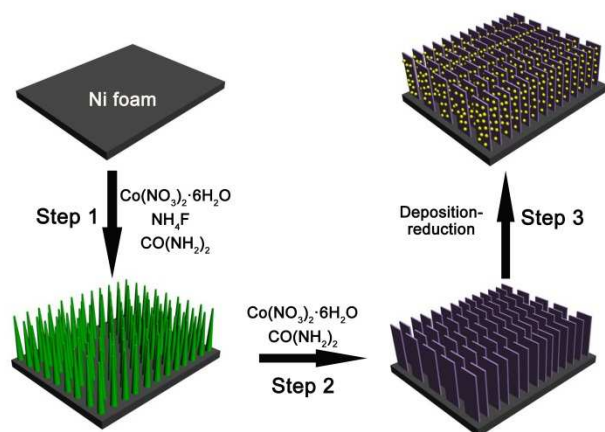
Powder X-ray diffraction (XRD) was performed on a Shimadzu XRD-6000 diffractometer with Cu Kα radiation (λ=1.5418 Å). The size and morphology of as-synthesized samples were characterized using scanning electron microscope (SEM, Zeiss Supra 55) with secondary electron imaging operating at 20 kV and transmission electron microscopy (TEM, Hitachi H-800) operating at 200 kV. The surface area analysis was determined by using an ASAP-2020 surface area analyzer. The samples were degassed at 453 K for 4 h prior to analysis. The Brunauer Emmett Teller (BET) method was utilized to calculate the specific surface areas. The pore size distributions (PSD) were derived from the desorption branch of the isotherm with the Barrett-Joyner-Halenda (BJH) method. The structure and composition of the products were characterized by means of a high-resolution transmission electron microscope (HRTEM, JEM 2100), energy dispersive X-ray spectroscopy (EDS) and X-ray photoelectron spectroscopy (XPS, ESCALAB 250). Samples for HRTEM were prepared by scraping the Au/ NiCoCH-NSAs from the substrate and ultrasonicing in ethanol, after which the suspension was dropped onto a carbon-enhanced copper grid and dried in air. Inductively coupled plasma (ICP) measurements were made on an inductively coupled plasma-atomic emission spectrometer (ICP-AES, Shimadzu ICPS-7500). UV-vis absorption spectra were measured at room temperature with a UV-2501PC UV-vis spectrophotometer (Shimadzu).

2.4 Catalyzed reduction of 4-NP

The reduction of 4-NP by Au/NiCoCH-NSAs in the presence of NaBH₄ was carried out to examine the catalytic activity and recyclability of the structured catalysts. Firstly, 4-NP with different concentrations (70 mL, 4.5×10⁻⁵ M - 2.5×10⁻³ M) was added to a 100 mL three-neck round bottom flask. Then, N₂ gas was purged through the solution for 30 min under continuous stirring condition to remove dissolved O₂. Subsequently, an aqueous solution of NaBH₄ (relative concentration of 4-NP to NaBH₄ is 0.012) was added. After the obtained Au/NiCoCH-NSAs on Ni substrate (2.0 cm×4.0 cm) was immersed in the above solution, the catalyzed reduction started. The progress of the reaction was monitored via UV-Vis spectroscopy by recording the time-dependent absorption spectra at a regular time interval of 2 min at room temperature.

3 Results and discussion

Au/bimetallic (Ni, Co) carbonate hydroxide nanosheet arrays (Au/NiCoCH-NSAs) on a nickel substrate were achieved by a two-step hydrothermal and deposition reduction method, as shown in Scheme 1. Firstly, bimetallic (Ni, Co) carbonate hydroxide nanowire arrays (NiCoCH-NWAs) vertical grown on the nickel foam were prepared by a facile hydrothermal reaction (Step 1). Then, uniform rectangular NiCoCH-NSAs were obtained by a secondary hydrothermal reaction of treating the as-prepared nanowire array with additional Co²⁺ salt and urea (Step 2). Afterwards, gold nanoparticles were deposited onto the NiCoCH-NSAs through a deposition reduction method using HAuCl₄ as the gold source (Step 3). The morphology evolution of the products was clearly revealed by the scanning electron microscopy (SEM). As shown in Fig. 1a, the obtained NiCoCH-NWAs are vertically grown on the substrates over a large scale.



Scheme 1 Schematic illustration of the fabrication procedures of Au/NiCoCH-NSAs.

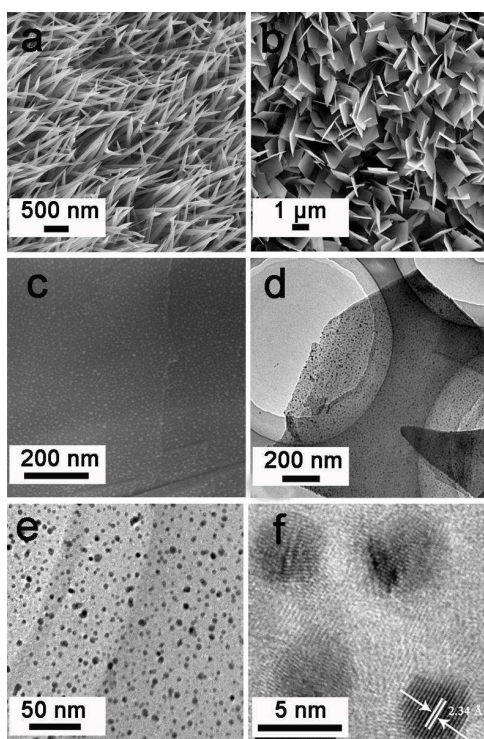


Fig. 1 (a, b) SEM images of NiCoCH-NWAs and NiCoCH-NSAs; (c-f) SEM (c), TEM (d and e) and HRTEM (f) images of obtained 2.8 wt% Au/NiCoCH-NSAs.

The vertical nanowires are about 50 nm in diameter and 2 μm in length. After the secondary hydrothermal reaction, NiCoCH-NWAs grew into uniform rectangular nanosheets, with an average width of ~1.5 μm, thickness of ~50 nm, and length of about several micrometers (Fig. 1b). In addition, the N₂ adsorption-desorption isotherm of NiCoCH-NSAs was provided in Fig. S1 †. The sample has a Brunauer-Emmett-Teller (BET) surface area of 61 m²/g which provides a high surface area to load and stabilize Au nanoparticles. Gold nanoparticles were uniformly loaded on the surface of nanosheets without aggregation over a large area by the deposition process, as shown in Fig. 1c. The size and distribution of gold nanoparticles on

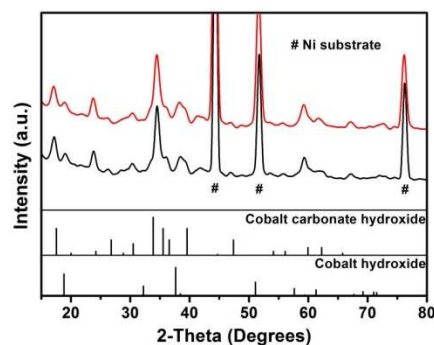


Fig. 2 XRD patterns of NiCoCH-NSAs (a) and Au/NiCoCH-NSAs (b). The inset bottom bars indicate the standard reflections from cobalt carbonate hydroxide (JCPDS No. 48-0083) and cobalt hydroxide (JCPDS No. 45-0031).

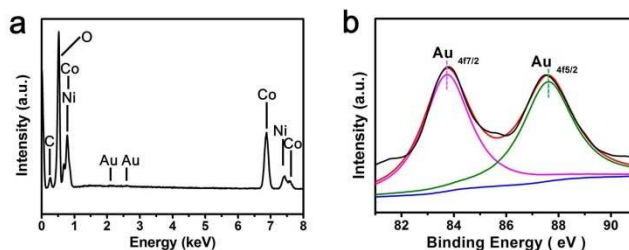


Fig. 3 (a) EDS spectrum and (b) Experimental and fitted Au 4f XPS spectrum for Au/NiCoCH-NSAs. The black line refer to the raw data, while the red line to the curve-fitting results.

Au/NiCoCH-NSAs were further studied by TEM and HRTEM. The results in Fig. 1d, e and Fig. S2 † showed that the size of the Au nanoparticles was about 2.6 nm ± 0.7 nm, further confirming the uniform distribution of the gold nanoparticles across the surface of the nanosheet. The clear lattice fringes ($d = 2.34 \text{ \AA}$) observed in the HRTEM image (Fig. 1f) agree well with the (111) lattice planes of the Au nanoparticles. Varying loading amount of Au, the morphologies of the nanosheet and the size of the Au nanoparticles in different samples were almost the same. The TEM images and size distribution of Au particles in Au/NiCoCH-NSAs with different gold loading amount were shown in Fig. S2 and the data were summarized in Table S1 as well. Au nanoparticles uniformly dispersed on the surface of the NiCoCH-NSAs without aggregation when the loading amount was less than 2.8 wt%. The slight agglomeration of Au nanoparticles only occurs when the loading amount was increased to 8.1 wt%.

XRD was used to characterize the phase of the as-synthesized product (Fig. 2). The main XRD peaks of the NiCoCH-NSAs can be assigned to cobalt carbonate hydroxide (JCPDS No. 48-0083). Small amount of cobalt hydroxide (JCPDS No. 45-0031) could also be detected.²⁶ It is worth pointing out that the XRD pattern of Au/NiCoCH-NSAs exhibited no detectable diffraction peaks of Au, which suggests the small size and high dispersion of the deposited Au nanoparticles. Energy dispersive X-ray spectroscopy (EDS) results, as shown in Fig. 3a, indicate the existence of Ni, Co components in the NiCoCH-NSAs (the atomic ratio of Ni/Co is around 1/6). The Ni²⁺ ions were generated from the dissolution of Ni foam in the starting acidic (pH = 6) and etching (containing F⁻ ions) solution. The existence of Au was measured by XPS and ICP. The XPS spectrum of 2.8 wt% Au/NiCoCH-NSAs displayed two obvious Au 4f peaks,

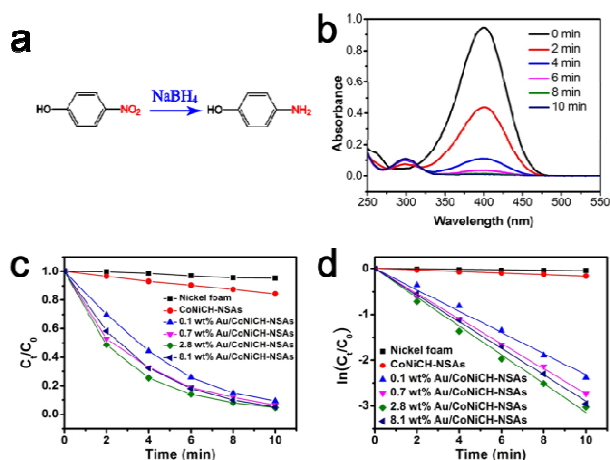


Fig. 4 (a) Schematic diagram of the catalytic reaction; (b) successive UV-vis spectra for the reduction reaction of 4-NP by NaBH_4 over 2.8 wt% Au/NiCoCH-NSAs; (c) C_t/C_0 and (d) $\ln(C_t/C_0)$ versus reaction time for the reduction of 4-NP over nickel substrate, NiCoCH-NSAs, 0.1 wt% Au/NiCoCH-NSAs, 0.7 wt% Au/NiCoCH-NSAs, 2.8 wt% Au/NiCoCH-NSAs and 8.1 wt% Au/NiCoCH-NSAs, respectively. C_0 and C_t was the absorption peak at 400 nm at initially and certain time t .

indicative of metallic Au at binding energies of 83.7 eV and 87.6 eV, in $\text{Au}_{4f_{7/2}}$ and $\text{Au}_{4f_{5/2}}$ levels,²⁷ confirming the complete in situ reduction of Au^{3+} ions by NaBH_4 , as shown in Fig. 3b. The ICP analysis indicated that the loading amount of Au is ca. 0.1 wt%, 0.7 wt%, 2.7 wt% and 7.8 wt% for 0.1 wt%, 0.7 wt%, 2.8 wt% and 8.1 wt% Au/NiCoCH-NSAs, respectively, which is close to the theoretical content (Table S1 †).

The catalytic reduction of 4-NP by NaBH_4 to produce 4-aminophenol (4-AP) was chosen as a probe reaction (Fig. 4a) to test the catalytic properties of Au/NiCoCH-NSAs. It is well-known that the 4-NP reduction by borohydride to 4-AP is of great significance, because 4-NP is a commonly used raw material and by-products in industries but with highly toxic for human beings since the long-term exposure may cause damages to blood cell, liver, and kidney.²⁸ By the addition of Au/NiCoCH-NSAs as catalyst, a typical UV-Vis absorption change of the reaction mixture appeared (Fig. 4b). The absorptions of 4-NP at 400 nm decreased with the concomitant increase of the 300 nm peak of 4-AP after the addition of catalyst. The UV-vis spectra also exhibited an isosbestic point between two absorption bands, indicating that only two principal species, 4-NP and 4-AP, influence the reaction kinetics.

To study the reduction rate of 4-NP over different catalysts, the evolution of the catalytic reduction reaction were monitored by recording the absorbance of 4-NP. Fig. 4c shows the C_t/C_0 versus reaction time for the reduction of 4-NP over NiCoCH-NSAs and Au/NiCoCH-NSAs with different amount of gold loading. For comparison, a blank test was conducted on nickel foam in the same reaction system. It could be observed that NiCoCH-NSAs showed low catalytic activity in reduction of 4-NP, a little better than nickel foam. In contrast, by loading of Au nanoparticles, a significant improvement in reduction of 4-NP was achieved. 2.8 wt% Au/CoNiCH-NSAs exhibited the highest catalytic activity, and 4-NP was effectively reduced within 8 min. Further increasing Au content to 8.1 wt%, however, the catalytic efficiency decreased. This might be attributed to the slightly

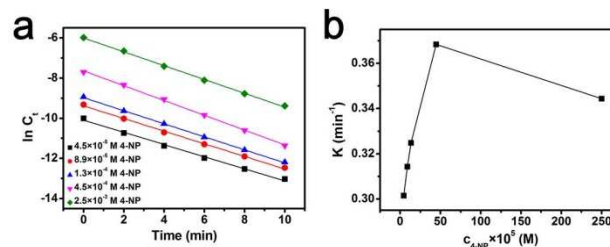


Fig. 5 (a) Catalytic activity of 2.8 wt% Au/NiCoCH-NSAs for different amount of 4-NP; (b) kinetic curves for the reduction of 4-NP catalyzed by 2.8 wt% Au/NiCoCH-NSAs.

aggregation of Au nanoparticles on the surface of NiCoCH-NSAs, resulting in the decrease of the number of active sites on the surface of the catalyst. In addition, the kinetic reaction rate (K) of the catalytic reaction was evaluated. Since excess NaBH_4 was used, the BH_4^- concentration remained essentially constant throughout the reaction, so pseudo-first-order kinetics could be applied for the evaluation of rate constants.²⁹ As expected, the linear relation of $\ln(C_t/C_0)$ versus time is observed for the catalysts, and the values of kinetic rate constant K can be calculated from the slope (Fig. 4d). Significantly, the K value for 2.8 wt% Au/NiCoCH-NSAs catalyst was calculated to be 0.30 min^{-1} , which is superior to many other Au-based catalysts under ambient conditions.^{30, 31}

In addition, further investigation on catalytic activity of Au/NiCoCH-NSAs for different concentration of 4-NP demonstrated that the Au/NiCoCH-NSAs has capability to maintain excellent catalytic activity even when the conversion of 4-NP was carried out on a relatively large scale such as a concentration of 2.5 mM 4-NP in a total solution volume of 70 ml. Fig. 5a shows the $\ln(C_t)$ versus reaction time for the reduction of 4-NP under different concentration of 4-NP. In each case, a linear correlation was found between $\ln(C_t)$ and reaction time. The corresponding value of K was calculated from the slope was plotted in Fig. 5b and also summarized in Table 1. It is found that, a nearly linear increase in the value of K was achieved as the concentration of 4-NP increased (Fig. 5b), when the concentration of 4-NP is lower than $4.5 \times 10^{-4} \text{ M}$. Further increasing the concentration of 4-NP would lead to a slight decrease of the catalytic efficiency. The explanation for this characteristic dependence of K on the concentrations of reactants was as follows.³² The catalytic reduction of 4-NP in the presence of an excess of NaBH_4 takes place on the surface of the particles where both species, namely 4-NP and surface-hydrogen species generated by borohydride ions (Langmuir-Hinshelwood kinetics).³³ Both reactants compete for free places at the surface of the Au nanoparticles. Therefore, when the concentration of 4-NP and NaBH_4 is relatively low and the surface is sufficient, an increase in the concentration of NaBH_4 leads to an increase in the reaction rate.³² However, if most places are occupied by 4-NP, the reaction will be slowed down considerably.^{32, 34} It is noteworthy that the kinetic reaction rate in a relatively high concentrations of 4-NP (2.5 mM) is larger than the literatures under ambient conditions.^{34, 35} Moreover, our experiment was carried out on a relatively large scale (70 mL of 4-NP), which is significantly greater than previous reports where micromolar

Table 1 The comparison of catalytic activity of Au/NiCoCH-NSAs (2.8 wt%) at different concentration of 4-NP and NaBH₄ with the ones reported in literature.

Type of catalysis	c _{4-NP} (M)	c _{NaBH₄} (M)	K (min ⁻¹)	Reference
Au/NiCoCH-NSAs	4.5×10 ⁻⁵	3.8×10 ⁻³	0.30	This work
	8.9×10 ⁻⁵	7.6×10 ⁻³	0.31	This work
	1.3×10 ⁻⁴	1.1×10 ⁻²	0.32	This work
	4.5×10 ⁻⁴	3.8×10 ⁻²	0.37	This work
	2.5×10 ⁻³	2.1×10 ⁻¹	0.34	This work
Spongy Au nanoparticles	1.0×10 ⁻⁴	1.0×10 ⁻²	0.13	30
Au nanoparticles/GO	3.5×10 ⁻³	8.0×10 ⁻²	0.19	31

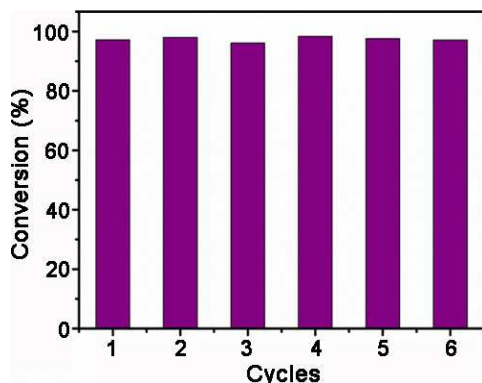
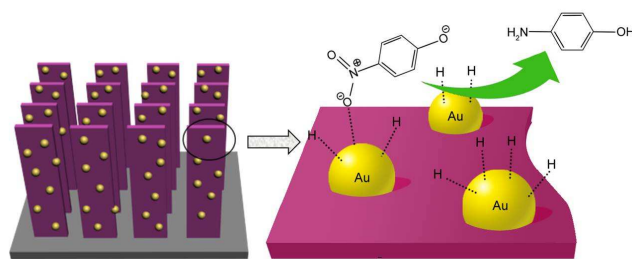


Fig. 6 The reusability of 2.8 wt% Au/NiCoCH-NSAs as catalysts for the reduction of 4-NP.

concentrations and a volume of a UV-visible cuvette of 3 mL were used.

Furthermore, the recyclability of the Au/NiCoCH-NSAs catalyst was also examined. After the reaction, the nanoarrays on the substrate were directly taken out from the reaction mixture and reused for the next run under the same conditions. The results demonstrated no significant loss of activity for the reduction of 4-NP over Au/NiCoCH-NSAs in the six successive catalytic cycles, indicating the long-term stability of the Au/NiCoCH-NSAs catalyst (Fig. 6). Such a good stability in catalytic activity is due to the good structural stability of NiCoCH-NSAs and the tight integration between Au nanoparticles and nanosheet arrays support (Fig. S3 †), finally producing an excellent catalyst with high activity and good reusability.

The high catalytic performance of Au/NiCoCH-NSAs could be attributed to the novel design of support materials of nanosheet array. In the reduction of 4-NP, the transmission and adsorption of 4-NP and surface-hydrogen species onto the catalyst surface,



Scheme 2 Possible mechanism for the catalytic reduction of 4-NP with the Au/NiCoCH-NSAs.

together with interfacial electron transfer and desorption of 4-AP from the surface have significant influence on the rate of the reaction.³⁶ As shown in Scheme 2, when Au/NiCoCH-NSAs were applied for the catalytic reduction, NaBH₄ and 4-NP were first diffused from aqueous solution to the surface of Au, and then the bare Au nanoparticles on nanosheets served as catalysts to transfer electrons from BH₄⁻ to 4-NP, leading to the production of 4-AP. Nanosheet arrays directly grown on the conductive substrates have inherent advantage in electronic transmission. In addition, the open space between nanosheets can facilitate the diffusion of active species. The thin nanosheet array of bimetallic (Ni, Co) carbonate hydroxide provides a high surface area to load and stabilize Au nanoparticles without aggregation, resulting to high rate of diffusion of active species which were in charge of the high catalytic activity.

4 Conclusions

In summary, Au/NiCoCH-NSAs as structured catalysts were synthesized by a two-step hydrothermal and deposition reduction method. The content of Au catalyst supported on nanosheet arrays could be well controlled by simply tuning the concentration of the whole reactants. The Au/NiCoCH-NSAs exhibited excellent catalytic activity and stability in the reduction of 4-NP, and the catalytic activity remains nearly unchanged even the reaction was carried out on a comparatively large scale, which was contributed to the structure of the nanosheet arrays and the large-scale uniformly distributed Au nanoparticles. In addition, the Au/NiCoCH-NSAs could be easily recycled from the product, greatly promoting their industrial application. Furthermore, this strategy can be extended to synthesize other supported catalyst on metallic substrates and offers new opportunities for the design of new types of highly efficient structured catalysts.

Acknowledgement

This work was financially supported by the NSFC, the Program for New Century Excellent Talents in Universities, Beijing Nova Program (Z121103002512023), Program for Changjiang Scholars and Innovative Research Team in University, the 863 Program (2012AA03A609) and the 973 Program (No. 2011CBA00503, 2011CB932403).

Notes and references

State Key Laboratory of Chemical Resource Engineering, Beijing University of Chemical Technology, Beijing 100029, China.
E-mail: ljf@mail.buct.edu.cn

Fax: +86-10-64425385; Tel: +86-10-64448751

† Electronic Supplementary Information (ESI) available: BET results, SEM results, TEM results of the catalyst and corresponding particle size distribution of Au. See DOI: 10.1039/b000000x/

- 1 T. K. Sau, A. L. Rogach, F. Jäckel, T. A. Klar and J. Feldmann, *Adv. Mater.*, 2010, **22**, 1805-1825.
- 2 D. J. Gorin, B. D. Sherry and F. D. Toste, *Chem. Rev.*, 2008, **108**, 3351-3378.
- 10 3 J. Zeng, Q. Zhang, J. Chen and Y. Xia, *Nano Lett.*, 2009, **10**, 30-35.
- 4 O. Vaughan, *Nat. Nanotechnol.*, 2010, **5**, 5-7.
- 5 Y. Sun and Y. Xia, *Science*, 2002, **298**, 2176-2179.
- 6 F.-h. Lin and R.-a. Doong, *J. Phys. Chem. C*, 2011, **115**, 6591-6598.
- 15 7 N. Zheng and G. D. Stucky, *J. Am. Chem. Soc.*, 2006, **128**, 14278-14280.
- 8 J. Shi, *Chem. Rev.*, 2013, **113**, 2139-2181.
- 9 X. Huang, C. Guo, J. Zuo, N. Zheng and G. D. Stucky, *Small*, 2009, **5**, 361-365.
- 20 10 P. Tribolet and L. Kiwi-Minsker, *Catal. Today*, 2005, **105**, 337-343.
- 11 P. Sonstroöm, M. Adam, X. Wang, M. Wilhelm, G. Grathwohl and M. Bäumer, *J. Phys. Chem. C*, 2010, **114**, 14224-14232.
- 25 12 J. Sun, Y. Li, X. Liu, Q. Yang, J. Liu, X. Sun, D. G. Evans and X. Duan, *Chem. Commun.*, 2012, **48**, 3379-3381.
- 13 L. E. Gómez, A. V. Boix and E. E. Miró, *Catal. Today*, 2013, **216**, 246-253.
- 30 14 A. Falase, M. Main, K. Garcia, A. Serov, C. Lau and P. Atanassov, *Electrochim. Acta*, 2012, **66**, 295-301.
- 15 K. Kuroda, T. Ishida and M. Haruta, *J. Mol. Catal. A: Chem.*, 2009, **298**, 7-11.
- 16 J. Li, C.-y. Liu and Y. Liu, *J. Mater. Chem.*, 2012, **22**, 8426.
- 35 17 K. LeeáTan, *J. Mater. Chem.*, 2001, **11**, 2378-2381.
- 18 K. Yu, Z. Wu, Q. Zhao, B. Li and Y. Xie, *J. Phys. Chem. C*, 2008, **112**, 2244-2247.
- 19 J. Jiang, J. Liu, R. Ding, J. Zhu, Y. Li, A. Hu, X. Li and X. Huang, *ACS Appl. Mater. Interfaces*, 2010, **3**, 99-103.
- 40 20 H. Chen, Y.-M. Yeh, J.-Z. Chen, S.-M. Liu, B. Y. Huang, Z.-H. Wu, S.-L. Tsai, H.-W. Chang, Y.-C. Chu and C. H. Liao, *Thin Solid Films*, 2013, **549**, 74-78.
- 21 Q. Yang, Z. Lu, Z. Chang, W. Zhu, J. Sun, J. Liu, X. Sun and X. Duan, *RSC Adv.*, 2012, **2**, 1663-1668.
- 45 22 X. Liu, J. Liu, Z. Chang, L. Luo, X. Lei and X. Sun, *RSC Adv.*, 2013, **3**, 8489.
- 23 Q. Yang, Z. Lu, J. Liu, X. Lei, Z. Chang, L. Luo and X. Sun, *Prog. Nat. Sci.: Mater. Int.*, 2013, **23**, 351-366.
- 24 C. Yuan, L. Yang, L. Hou, L. Shen, X. Zhang and X. W. Lou, *Energy Environ. Sci.*, 2012, **5**, 7883.
- 50 25 K. Kuroda, T. Ishida and M. Haruta, *J. Mol. Catal. A: Chem.*, 2009, **298**, 7-11.
- 26 W. Zhu, Z. Lu, G. Zhang, X. Lei, Z. Chang, J. Liu and X. Sun, *J. Mater. Chem. A*, 2013, **1**, 8327.
- 55 27 Z. Bian, J. Zhu, F. Cao, Y. Lu and H. Li, *Chem. Commun.*, 2009, **0**, 3789-3791.
- 28 H. Xiao, Y. Xia and C. Cai, *J. Nanopart. Res.*, 2013, **15**, 1521.
- 29 J. Lee, J. C. Park and H. Song, *Adv. Mater.*, 2008, **20**, 1523-1528.
- 60 30 H. MdRashid, R. R. Bhattacharjee, A. Kotal and T. K. Mandal, *Langmuir*, 2006, **22**, 7141.
- 31 Y. Zhang, S. Liu, W. Lu, L. Wang, J. Tian and X. Sun, *Catal. Sci. Technol.*, 2011, **1**, 1142-1144.
- 32 P. Hervés, M. Pérez-Lorenzo, L. M. Liz-Marzán, J. Dzubiella, Y. Lu and M. Ballauff, *Chem. Soc. Rev.*, 2012, **41**, 5577.
- 65 33 J. Kaiser, L. Leppert, H. Welz, F. Polzer, S. Wunder, N. Wanderka, M. Albrecht, T. Lunkenbein, J. Breu and S. Kümmel, *Phys. Chem. Chem. Phys.*, 2012, **14**, 6487-6495.
- 34 S. Wunder, Y. Lu, M. Albrecht and M. Ballauff, *ACS Catal.*, 2011, **1**, 908-916.
- 70 35 S. Wunder, F. Polzer, Y. Lu, Y. Mei and M. Ballauff, *J. Phys. Chem. C*, 2010, **114**, 8814-8820.
- 36 S. Jana, S. Ghosh, S. Nath, S. Pande, S. Praharaj, S. Panigrahi, S. Basu, T. Endo and T. Pal, *Appl. Catal. A: Gen.*, 2006, **313**, 41-48.
- 75

Graphical Abstract:

A novel structured catalyst, Au/bimetallic (Ni, Co) carbonate hydroxide nanosheet arrays, supported on a three-dimensional substrate were prepared, which exhibited excellent catalytic activity for the reduction of p-nitrophenol (4-NP).

